Surface Normal Modes of Lake Michigan: Calculations Compared with Spectra of Observed Water Level Fluctuations

DESIRAJU B. RAO,[1] C. H. MORTIMER[2] AND DAVID J. SCHWAB[1]

(Manuscript received 25 September 1975, in revised form 23 February 1976)

ABSTRACT

Periods and structures of several normal modes of Lake Michigan (including Green Bay) are calculated theoretically, taking into account the Lake's topography and the earth's rotation. The calculations are based on a Galerkin method developed by Rao and Schwab (1976). Even though the calculations give both rotational and gravitational modes, attention is focused primarily on the latter. The calculations show that there are several modes dominant in the main basin of Lake Michigan and some dominant in Green Bay. The lowest Lake Michigan mode has a period of 9.27 h. Green Bay exhibits a (co-oscillating or Hemlholtz) mode with a period 10.35 h. For the modes dominant in the main basin, the periods and structures obtained from theoretical calculations are compared to those deduced from spectral analyses of water level data from various stations around the Lake. The agreement is found satisfactory for several of the lowest modes.

1. Introduction

The problem of two-dimensional barotropic normal modes of Lake Michigan is considered here. Past studies of free oscillations in Lake Michigan and other water bodies have dealt with the one-dimensional channel theory, an excellent summary of which is contained in Defant (1961). Channel theory, though fairly successful for the lowest longitudinal modes, breaks down for higher modes and for bodies of water that are not "narrow and elongated." It is only recently that the two-dimensional problem of free oscillations in natural water bodies, taking into account the earth's rotation, has been successfully attacked (see, for example, Platzman, 1972, 1975). In this paper, frequencies and structures of the two-dimensional normal modes are calculated theoretically by the method briefly described later, and the results are compared with observations of the gravitational modes wherever possible.

2. Governing equations and the method of calculation

We are concerned with the small-amplitude, free, quasi-static oscillations of a homogeneous lake on a rotating earth. The governing equations are the familiar Laplace's "tidal" equations. If $\mathbf{V}$ is the horizontal velocity vector and η the free surface displacement from the equilibrium position, these equations may be written as

$$\frac{\partial \mathbf{a}}{\partial t} = L\mathbf{a}, \tag{1}$$

where

$$\mathbf{a} \equiv \begin{pmatrix} \mathbf{M} \\ \eta \end{pmatrix},$$

$$L \equiv \begin{pmatrix} -f\mathbf{k}\times & -gH\nabla \\ \nabla\cdot & 0 \end{pmatrix}.$$

In the above equations the dependent variable is taken as the transport vector $\mathbf{M} \equiv H\mathbf{V}$ instead of the velocity vector $\mathbf{V}$. $H(x,y)$ is the equilibrium depth of the lake. The symbols defined in the spatial differential operator L have their usual meaning. If we consider the lake to be a fully enclosed water body, then the appropriate boundary condition to be imposed on (1) is the adiabatic condition

$$\mathbf{M}\cdot\mathbf{n} = 0 \tag{2}$$

on the coastline, where $\mathbf{n}$ is a unit vector normal to the coast.

In order to determine the normal modes, we seek a simple-harmonic solution, $\mathbf{a} = \mathbf{A}e^{i\sigma t}$, so that Eq. (1) becomes

$$L\mathbf{A} = i\sigma\mathbf{A}. \tag{3}$$

It is clear that the frequencies σ (multiplied by $i \equiv \sqrt{-1}$) are the eigenvalues of the operator L and the $\mathbf{A}$'s are the corresponding eigenvectors. Each eigenvector $\mathbf{A}$ is a function of the horizontal coordinates and represents

[1] Great Lakes Environmental Research Laboratory, NOAA, Ann Arbor, Mich. 48104. Contribution No. 42.

[2] Center for Great Lakes Studies, The University of Wisconsin-Milwaukee, Milwaukee, Wisc. 53201. Contribution No. 148.

the spatial structure of a normal mode associated with a particular frequency σ.

The solution to the operator equation (3) must proceed by discretising the operator L, particularly when a real lake with arbitrary bathymetry and planform is considered. Platzman (1975) lucidly discusses the various methods considered by different investigators to attack the problem. The method adopted here is a Galerkin method described by Rao and Schwab (1976). This method proceeds in three steps. Steps 1 and 2 consist of numerically constructing two sets of orthogonal functions, one set for the irrotational part of the velocity field and the other for the solenoidal part of the transport field by solving two self-adjoint elliptic operators:

STEP 1

$$\left.\begin{aligned} &\nabla\cdot H\nabla\phi_\alpha=-\lambda_\alpha\phi_\alpha \\ &H\frac{\partial\phi_\alpha}{\partial n}=0 \text{ on the boundary} \end{aligned}\right\} \tag{4a}$$

STEP 2

$$\left.\begin{aligned} &\nabla\cdot H^{-1}\nabla\psi_\alpha=-\mu_\alpha\psi_\alpha \\ &H^{-1}\psi_\alpha=0 \text{ on the boundary} \end{aligned}\right\} \tag{4b}$$

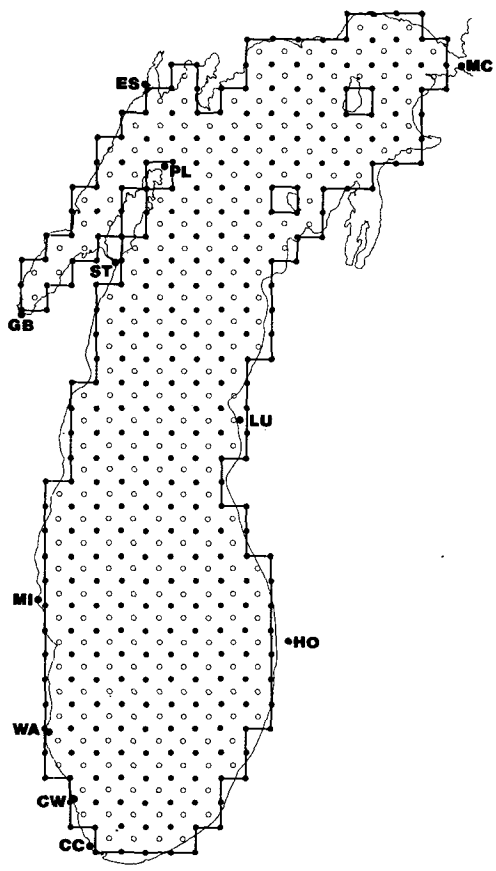

FIG. 1. Map of Lake Michigan with the computational grid superimposed. Code letters refer to water level recording stations listed in Table 2.

Here ϕ_α, ψ_α are the velocity potential and the transport streamfunction and λ_α, μ_α are the characteristic values of the above self-adjoint problems. If there are no Coriolis forces in the equations, the solutions of the solenoidal part (step 2) represent circulation associated with nondivergent transports and those of the irrotational part (step 1) represent no-rotation, free gravitational oscillations of the basin. When Coriolis forces are present, these two fields are coupled as shown by Proudman (1916) and the solutions to the rotating problem [Eq. (3)] are built up by superposition of these two sets of orthogonal functions (step 3). That is, the dependent variables of the rotating case are expressed as

STEP 3

$$\left.\begin{aligned} \mathbf{M}^\phi&=\sum_\alpha p_\alpha\mathbf{M}_\alpha^\phi \\ \mathbf{M}^\psi&=\sum_\alpha q_\alpha\mathbf{M}_\alpha^\psi \\ \eta&=\sum_\alpha r_\alpha\eta_\alpha \end{aligned}\right\}, \tag{5}$$

where $\mathbf{M}\equiv\mathbf{M}^\phi+\mathbf{M}^\psi$. The functions $\mathbf{M}_\alpha^\phi$ and $\mathbf{M}_\alpha^\psi$ and η_α are given by

$$\mathbf{M}_\alpha^\phi=-H\nabla\phi_\alpha;\ \mathbf{M}_\alpha^\psi=-\mathbf{k}\times\nabla\psi_\alpha;\ \eta_\alpha=\left(\frac{\lambda_\alpha}{g}\right)^{\frac{1}{2}}\phi_\alpha. \tag{6}$$

When these expansions are substituted into the rotating problem and use is made of the orthogonality of the basis functions ϕ_α, ψ_α, we obtain a matrix representation of the operator L [Eq. (3)]. The eigenvector $\mathbf{A}$ in that equation is the set of expansion coefficients $(p_\alpha,q_\alpha,r_\alpha)$ defined in (5) for an eigenfunction of the rotating case.

The free oscillations in an arbitrary rotating basin constitute two distinct types of modes, gravitational and rotational. The existence of gravitational modes is entirely dependent on free surface undulations; they can exist even if there is no rotation (Coriolis forces). In the absence of rotation, the gravity modes are standing waves with nodal lines, across which the phase of the wave changes discontinuously through 180°. When rotation is taken into consideration, the standing modes are transformed into propagating modes and the nodal lines are replaced by amphidromic points. The rotational modes owe their existence solely to deformations of potential vorticity f/h in the undisturbed state (produced by topographic gradients in a homogeneous lake with a constant f) and they can exist in the absence of gravity. Their structures are dominantly quasi-horizontal. Apart from these distinctions, there is another fundamental distinction between the rotational and gravitational modes. The periods of most gravitational modes are less than those of most rotational modes. For the Great Lakes of North America, the frequencies of all gravitational modes are generally confined to the range $f<\sigma<\infty$ and the frequencies of the rotational modes to the range

TABLE 1. Frequencies and features of the first 13 normal modes of the main basin of Lake Michigan (not including Green Bay modes) calculated with rotation.*

Frequency (cpd)	Equivalent period (h)	Principal features	Later identification with observed oscillations (cpd)
2.59	9.27	see Fig. 4a	2.66
4.57	5.25	see Fig. 4b	4.61
6.30	3.81	see Fig. 5a	6.51
7.61	3.15	see Fig. 5b	7.70
8.86	2.71	Maximum range at far N end around negative amphidrome.	8.87 peak at MC only
9.55	2.51	see Fig. 6a	9.51
10.55	2.28	see Fig. 6b	10.94
10.65	2.25	Range maxima at extreme N end and SW corner, the latter associated with a negative amphidrome.	component of (?) 10.94
11.39	2.11	Range 100% near Escanaba (Green Bay) and 36% at Chicago.	none seen
11.96	2.01	Two positive, four negative amphidromic systems. Highly complex.	12.00[a]
12.61	1.90	Seven amphidromic regions (two negative); amplitudes greates in S half.	12.52(g)[b]
13.27	1.81	Both modes (13.27 and 13.61) show: complicated structures; highest ranges near Beaver Island and Chicago; isolated pockets>20% elsewhere; seven nodal lines in corresponding velocity potential functions.	none seen
13.61	1.76		13.61(h)[b]

* Only the structures of the five lowest modes are shown in this paper. The authors intend to describe the structures of higher modes in a Special Report, Center for Great Lakes Studies, University of Wisconsin-Milwaukee.

[a] Only at CC (f_1 in Fig. 2).

[b] Lettered peaks in Figs. 2 and 3.

$0<\sigma<f$. (In the continuum, zero frequency is a condensation point for rotational modes as is infinite frequency for gravitational modes.) These differences in the two types of modes become important when the question of verification of theoretical calculations with observations is considered. In the present investigation, the verification of the calculations is based on analyses of water level data (details are given later), and from these analyses it is only possible to focus attention on the gravitational modes of oscillation.

The structures of the normal modes discussed later are given in terms of the variations of the height field $\eta(x,y,t)$. The solution for a normal mode of frequency σ may be written as

$$\left.\begin{aligned}\eta(x,y,t)&=\mathrm{Re}\{\eta(x,y)e^{i\sigma t}\}\\&\equiv\hat{A}(x,y)\cos[\sigma t-\theta(x,y)]\\\hat{A}&\equiv(\eta_r^2+\eta_i^2)^{\frac{1}{2}}\\\theta(x,y)&=\arctan\left(-\frac{\eta_i}{\eta_r}\right)\end{aligned}\right\}. \qquad (7)$$

Here $\hat{A}$ is the amplitude with its isopleths representing co-range lines, and θ is the phase of high water with its isopleths representing co-tidal lines.

3. Lake Michigan basin

The calculations for the frequencies and structures of normal modes are carried out using grid squares of 14.4 km side fitted to the outline of Lake Michigan, including Green Bay (Fig. 1). The depths are given at appropriate points. The mean depth of the Lake from the numerical grid, 84.2 m, is 1.3% less than that derived from Lake depth charts. The influence of this difference on calculated frequencies will be noted later. The dots, indicating the positions where the transport stream-functions are defined, and the open circles, indicating the points where the velocity potentials are defined, total 200 points for the streamfunction and 271 for the velocity potential. Thus, by solving Eqs. (4a, b) in the discretised form on their respective grids, we obtain 200 orthogonal functions (ψ_α's) for the solenoidal field and 271 (ϕ_α's) for the irrotational field. In the final step, the number of ϕ_α and ψ_α functions to be used in the superposition [Eqs. (5)] for the rotating solution is arbitrary. Here we arrange the ϕ_α's and ψ_α's in such a fashion that the associated λ_α's and μ_α's [see Eq. (4)] form an ascending sequence and use the lowest 50 of the ϕ_α's and ψ_α's. Such a choice of truncation of the above basis functions retains the ones with the largest space scales, and the resulting eigenvalues and eigen-functions of the rotating problem converge rapidly—at

least for the gravitational modes. The calculation provides for each mode: (i) a frequency; (ii) a phase angle for each grid point, relative to 0° at the grid point corresponding to Mackinaw City (MC in later diagrams); and (iii) the distribution of elevation range relative to 100 at whichever grid point possessed maximum range for that particular mode. From (ii) and (iii) the co-phase (co-tidal) lines and co-range lines were interpolated (see Figs. 4–7).

4. The first 13 normal modes of the main basin, calculated with rotation and compared with spectra of observed fluctuations in water level

We found two distinct types of range distribution: one in which the largest ranges are confined to Green Bay, with less than 10% elsewhere in the main basin, and a second type in which the largest ranges are in the main basin. For convenience we shall refer to these two types as Green Bay modes and main basin modes, respectively, although both contribute to the complete set of *whole* basin modes. We describe and discuss the Green Bay modes in a later section.

The frequencies (and periods) of the first 13 normal modes of the main basin, calculated with rotation, are listed in Table 1 with descriptive remarks and with the corresponding frequencies of observed oscillations with which the calculated modes were identified. To avoid later confusion, which a sequential numbering scheme might introduce, the modes are referred to by their *calculated* frequency in cycles per day (cpd). Table 1 discloses that the observed frequencies are generally slightly higher than those calculated. The percentage differences range from −0.7 to +3.5 and average +1.4. The mean depths computed for the model and for the Lake when the water levels were recorded (chart depth plus 0.3 m) were 84.2 and 85.3 m, respectively, with square roots differing by 0.7%. This accounts for part of the difference between computed and observed frequencies.

TABLE 2. Code letters used for the water level recording stations around the Lake (see Fig. 1).

Station name	Code letters
Mackinaw City, Mich.	MC
Sturgeon Bay Canal, Wis.	ST
City of Green Bay, Wis.	GB
Milwaukee, Wis.	MI
Waukegan, Ill.	WA
Wilson Avenue Crib, Chicago, Ill.	CW
Calumet Harbor, Ill.	CC
Holland, Mich.	HO
Ludington, Mich.	LU
* Escanaba, Mich.	ES
* Plum Island, Wis.	PI

* The recorders at these stations were operated for a short period of time only.

For comparison with calculated frequencies and structures, spectra of water level fluctuations at coastal stations are used. Table 2 lists the names of these stations and the code letters adopted for convenience. Particulars of the recorders and of the agencies operating them are given in the papers quoted later in this section. The spectra used to obtain frequency and structure were derived from three sets of water level data with the mean and best-fitting linear trend removed: (a) two months (July-August 1961 or November-December 1962) of 15 min averages of water levels estimated by eye and digitized from continuous traces; (b) eighteen months (June 1962 to November 1963) of hourly, non-averaged readings digitized by the U. S. Army Corps of Engineers, Lake Survey, from original charts; and (c) six months of 5 min readings (May-November 1969) from stations ST, GB and LU, also supplied by the U. S. Lake Survey (see Acknowledgments). Portions of data sets (a) were used to prepare the spectra for single stations in Mortimer (1965). Data sets (b) and (c) were used to prepare the spectra in Mortimer and Fee (1976) in which station pairs were analyzed for coherence and phase difference. That paper should be consulted for detailed descriptions of the methods used and of the way in which aliasing difficulties were circumvented. The first six main Lake modes were identified as five longitudinal modes of the whole basin and a uninodal transverse oscillation of the southern half. The phase progressions of the first two longitudinal modes and of the semidiurnal tide were determined. Much of the interstation coherence and phase information obtained during that study could not be used because seven recording stations (CW and WA were not included) were too few to "resolve" the phase progressions of modes above the second. Now that the calculated structures are available, further progress can be made.

The 1961–62 spectra, not severely aliased because 15 min average levels were used, are plotted on a common frequency scale covering 0 to 28 cpd in Figs. 2 and 3 for the main basin. The complete spectral range was 0 to 48 cpd, but few features of interest were found above 28 cpd. As we are here principally interested in frequencies and structures, the absolute scaling of spectral density is not included. Relative heights of spectral peaks are sufficient for our purpose.

First we identified peaks, some prominent, some less so, which appear at or close to the same frequency in spectra from several stations. These are indicated by best-fit vertical lines in Figs. 2 and 3. We have used letter labels to provide continuity with Mortimer and Fee's (1976) discussion. Where slight differences were found between the frequency estimates so derived and those published by Mortimer and Fee, we use (in Tables 1 and 3) the estimates from Figs. 2 and 3 because of the greater resolution of the 1961–62 spectra.

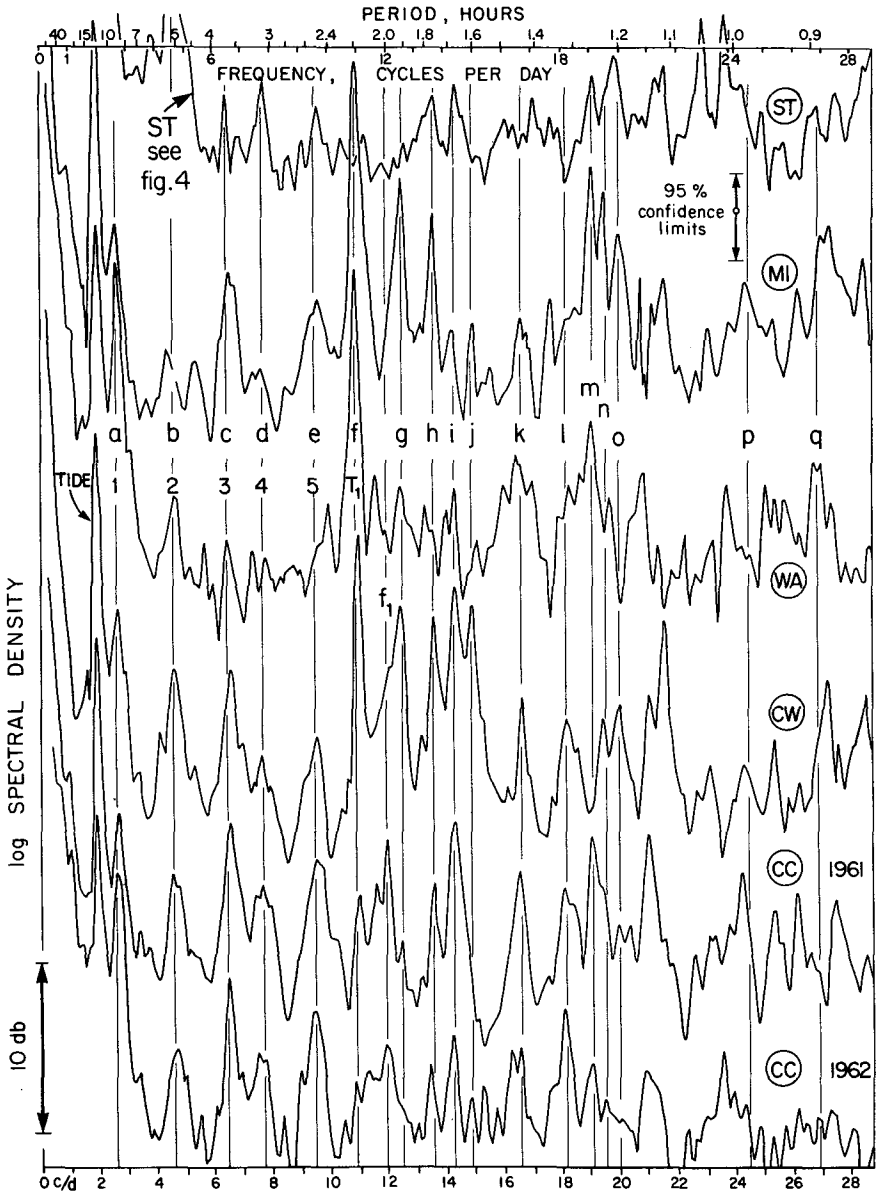

FIG. 2. Spectra of water level fluctuations derived from two months of 15 min average levels at recording stations around the shores of the main Lake Michigan basin in July–August 1961 or November–December 1962: ST (1962), MI (1961), WA (1962), CW (1961) and CC (1961, 1962). The letters used to indicate spectral peaks are also used in Figs. 3 and 9; each vertical line is a best fit to peaks occurring near this frequency in several spectra, definining an "observed" oscillation.

A rough indication of amplitude distribution among the stations is given by inspection of heights of spectral peaks in Figs. 2 and 3. The following code was used for the comparisons in Table 3 and in Figs. 4–6: *** very large, ** large, * present, *⁻ present but small, *0 not visible. Estimates of the phase progression of the observed modes followed the procedure described by Mortimer and Fee (1976) and used unpublished information on interstation coherence and phase, extracted from the 1962–63 and 1969 spectra. All interstation phase differences were used to derive the best fit of station angles relative to 0° at MC, giving greatest weight to those estimates associated with high interstation coherence. For the lowest mode, the scatter of interstation phase estimates for individual station pairs around the best fit was small (±3° or +7°−6° if GB 1969 was included). The scatter was greater for the higher modes (see Table 3). The scatter for the fifth and higher modes was too great to yield useful comparisons.

The structures of six of the lowest modes computed for the main basin (i.e., not including Green Bay modes) are assembled in Figs. 4–6 and are referred to by their calculated (with rotation) frequencies. Modes 2.59, 4.57 (Fig. 4) and 6.30, 7.61 (Fig. 5) and 9.55 (Fig. 6a) are counterparts of longitudinal modes 1 to 5 identified by Mortimer and Fee (1976), with one to five positive amphidromic regions, i.e., with counterclockwise phase progression (a filled circle represents a positive amphidromic point). Mode 10.55 in Fig. 6b corresponds with the first transverse mode of the southern half of the Lake, described and named T_1 in Mortimer's previous publications (e.g., 1965). As theory predicts (Rao, 1966), the transverse oscillation is associated with a negative amphidrome (an open circle represents a negative amphidromic point). This occupies most of the southern half of the basin and is associated with large-amplitude ranges. When, as in this case, the calculations show an extensive amphidromic system, large oscillations are seen in the spectra.

The "observed" spectral evidence for these identifications is entered on lines B and D in Table 3 and in Figs. 4–6. As explained in the legend of Fig. 4 and in the heading of Table 3, the observed quantities are estimates of frequency, relative elevation range at individual stations, and station phase angle. The calculated values are entered for comparison on lines A and C of the Table. They correspond to single grid

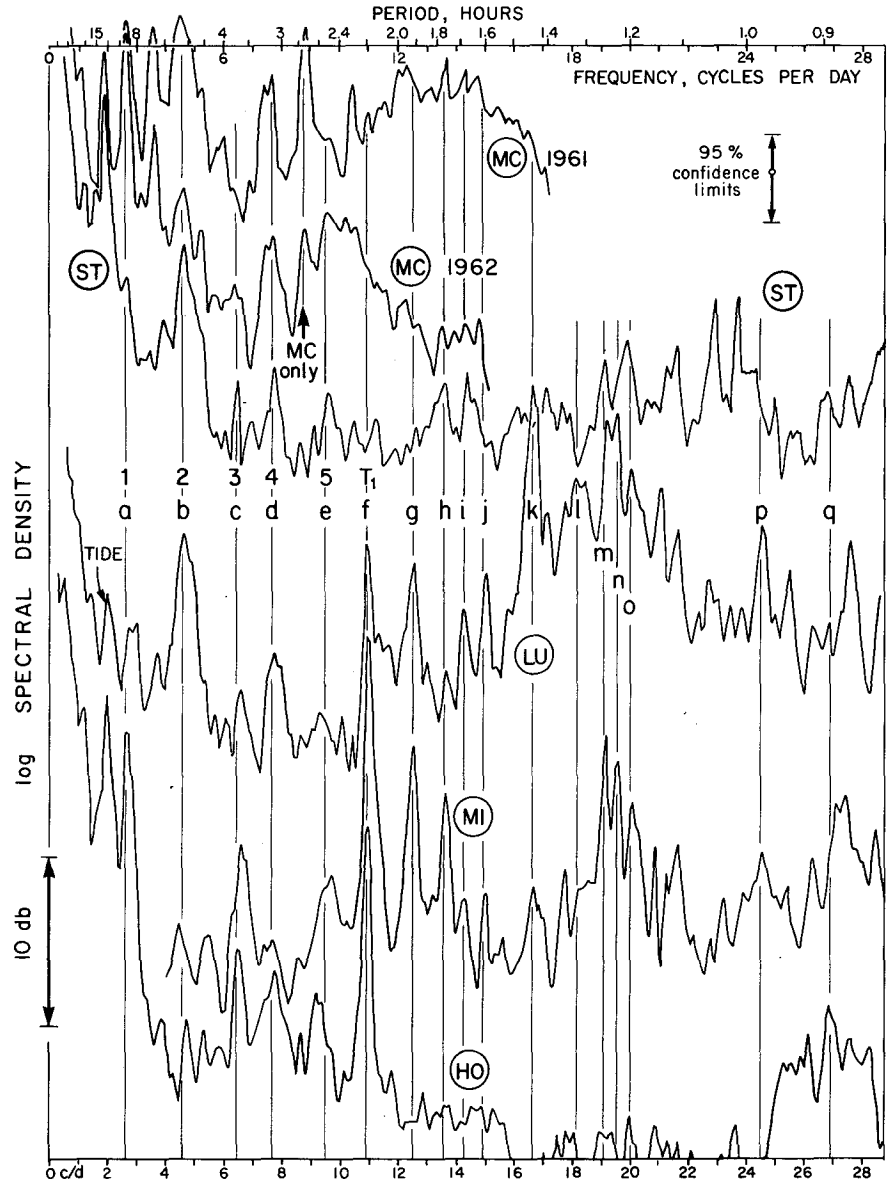

FIG. 3. As in Fig. 2 except for MC (1961, 1962), ST (1962), LU (1961), MI (1961) and HO (1962).

TABLE 3. Comparisons of calculated and observed frequencies, elevation ranges and phase angles for five main basin modes and nine stations (explanation of the line headings given at the bottom of the Table).

Mode (cpd)	Station	MC	ST	MI	WA	CW	CC	HO	LU	GB	Maximum deviation	
2.59												
[2.66][a]	A	100	29	35	56	64	66	46	4	94		
	B	**	*	*	**	*	**	**	*—	***		
	C (deg)	0	3	177	178	179	180	183	320	193		
	D (deg)	0	—	151	—	—	169	197	294	166	+7	−6
	E (deg)	0		+26			+11	−14	+26	+27		
4.57	A	100	33	5	23	35	38	9	33	70		
[4.61]	B	**	***	*0	*	**	**	*—	***	**		
	C (deg)	0	177	203	353	357	359	17	175	164		
	D (deg)	0	150		—	—	310	30	170	100	+13	−19
	E (deg)	0	+27				+49	−13	+5	+64		
6.30	A	100	5	25	16	48	60	12	23	28		
[6.51]	B	*0	*—	**	*—	**	***	*	*—	*		
	C (deg)	0	200	12	163	181	186	347	11	26		
	D (deg)	0	150	355	—	—	170	25	46	225	+12	−12
	E (deg)	0	+50	+17			+16	−38	−35	+161		
7.61	A	83	36	34	13	72	100	36	23	5		
[7.70]	B	**	*	*—	*0	*	**	*	*	*0		
	C (deg)	0	4	185	269	355	4	180	354	245		
	D (deg)	0	350	135	—	—	330	215	310		+30	−29
	E (deg)	0	+14	+50			+34	−35	+44			
10.55	A	78	3	6	51	33[b]	20	19	7	1		
[10.94]	B	*0	*0	***	***	***	*—	***	**	*0		
	C (deg)	0	222	268	241	253	79	50	208	28		
	D (deg)	0		250	—	—	100	227	55		+17	−17
	E (deg)	0		+18			−21	−177	+153			

[a] "Observed" frequencies on line B may differ slightly from those published by Mortimer and Fee (1976) because they were derived from 1961–62 and 1962–63 spectra, respectively.

[b] Elevation range (100) occurs on the shore line between WA and CW.

The left-hand column lists, for the mode considered, the calculated and observed frequencies shown without and with square brackets, respectively. Line headings are as follows:

A. Calculated elevation range at each station point, relative to a basin maximum of 100.
B. Approximate categorization, for each station, of the magnitude of the spectral peak lying at or close to the observed frequency (by inspection of Figs. 2 or 3). The following code is used: *** very large, ** large, * present, *− present but small, *0 not visible. The code allocation depends, not only on modal structure, but also on how strongly the particular mode is excited.
C. Calculated phase angle at each station point, relative to 0° at MC.
D. "Observed" phase angle, for each station and relative to 0° at MC, derived in the manner described in the text. The "odserved" phase angle is omitted where the spectral peak is not visible (code *0 in column B). Maximum deviation is that of indivibual station pairs from the best fit for all stations pairs.
E. Calculated phase angle minus observed phase angle, i.e. C−D.

points for stations GB, MI, CC, HO and LU. Stations ST, WA and CW are better represented by the average values of pairs of grid points. Notes follow on individual main basin modes, referred to by their calculated frequencies.

a. Mode 2.59 cpd (first longitudinal mode)

Fig. 4a shows two positive amphidromes, one occupying the whole main basin, the other inside the mouth of Green Bay. The agreement with observed amplitude distribution and phase progression is relatively close, the maximum spread of the differences in line E, Table 3, being only 41°. This lowest main basin mode, with a large amplitude range (94) at GB, is one of the driving oscillations for the Green Bay resonance, the semidiurnal tide being the other.

b. Mode 4.57 cpd (second longitudinal mode)

Fig. 4b shows four positive amphidromes, two occupying the main basin, one at the mouth, and one near the inner end of Green Bay.

Whereas the peaks corresponding to the first mode are apparently single, the second mode appears incorporated in a double peak in many spectra (spectra CC, WA, LU and MC in Figs. 2 and 3) with summits near 4.6 and 4.8 cpd. The origins of this double peak

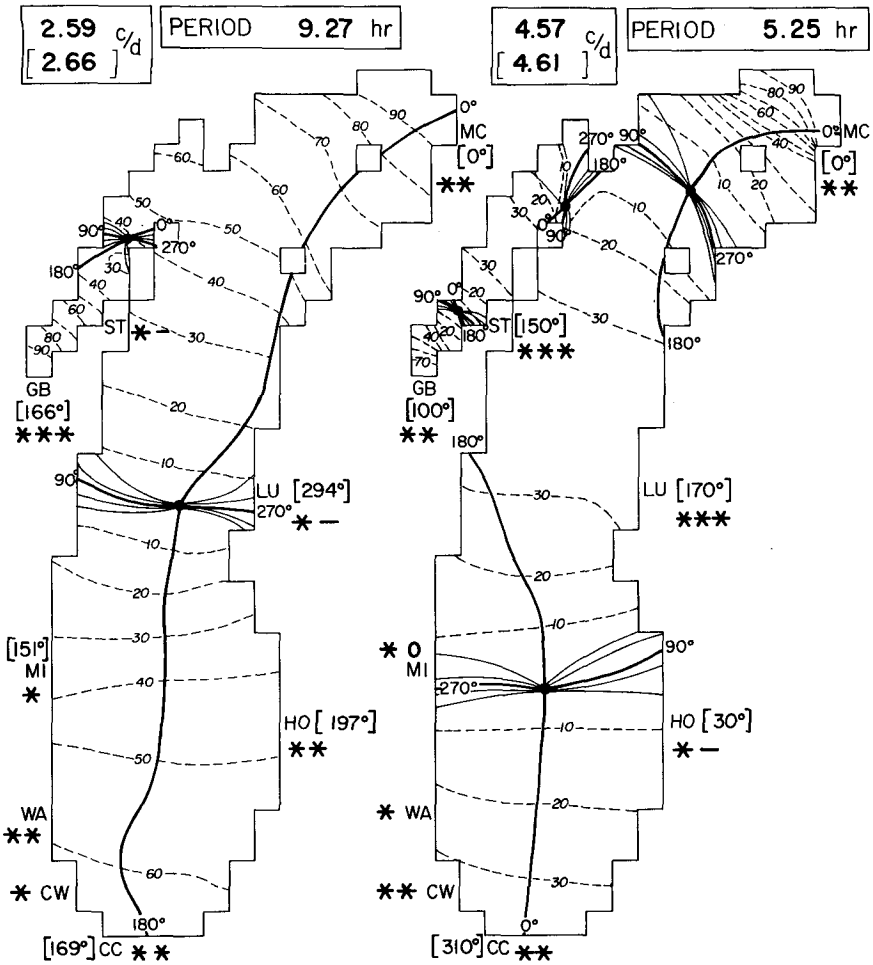

FIG. 4. Calculated frequency, period and structure of the first two longitudinal modes of the main Lake Michigan basin, taking the earth's rotation into account. Phase progression, relative to 0° at MC, is shown by co-tidal lines (heavy for 0°, 90°, 180° and 270°, light for 30° intervals). Distribution of relative elevation range is shown by co-range lines, broken and relative to 100 at that grid point which exhibits maximum range for the mode concerned. The bracketed "observed" frequency at the head of the figure is that of the particular spectral peak (Figs. 2 and 3) identified with the calculated mode. Bracketed angles near some station code letters are the "observed" phase angles, for the "observed" oscillation and relative to 0° at MC, derived for those stations from interstation coherence and phase information as described in the text. The asociated coding categorizes the spectral heights at the "observed" frequency in Figs. 2 and 3: *** very large; ** large; * present; *– present but small; *0 not visible.

were discussed by Mortimer and Fee (1976, their Fig. 8). They tentatively identified the second Michigan mode at 4.8 cpd and interpreted 4.6 cpd as the signal from a co-oscillation with Lake Huron, with which the Michigan basin is connected through the Straits of Mackinac. In reality the combined Michigan-Huron basin will possess a complete set of normal modes, with a Michigan and a Huron subset strongly developed in one basin but not in the other. It is also likely that some modes possess appreciable amplitudes in both basins; but because our model is closed at the Straits, these modes are excluded.

Table 3 shows good agreement between the phase progressions of the calculated 4.57 cpd mode and the observed oscillation at 4.61 cpd. The greatest deviation in the main basin is at MI where the elevation amplitude is very low. Agreement between the elevation amplitudes is also good; and oscillation b in Figs. 2 and 3 must therefore be identified with the second Michigan longitudinal mode, contrary to the earlier opinion of Mortimer and Fee (1976). This leaves the identity of the 4.8 cpd oscillation unclear. We have confirmed that it is not a good fit, in phase progression or amplitude distribution, to the second Green Bay mode at 4.84 cpd (see Table 4). Perhaps it is a Michigan-Huron mode.

c. Mode 6.30 cpd (third longitudinal mode)

Except at MI, the spectral peaks at 6.51 cpd identified with this mode appear to be single, and (except at GB) this identity is well supported by Table 3. Fig. 5a shows three positive amphidromes in the main basin and three in Green Bay.

d. Mode 7.61 cpd (fourth longitudinal mode)

With three positive amphidromes in Green Bay and four in the main basin (Fig. 5b), this mode shows good agreement (Table 3, except for GB phase angle) with the observed 7.7 cpd oscillation. However, the peak summit at this frequency appears as a component of a multiple (triple?) peak in several spectra (CC, MI, LU and MC, Figs. 2 and 3). Again Michigan-Huron oscillations may be involved.

e. Mode 9.55 cpd (fifth longitudinal mode)

This mode is characterized (Fig. 6a) by five positive amphidromes in the main basin, with the main activity associated with the most northerly and the most southerly of these. There are also five amphidromes in Green Bay, two of which are negative. The observed oscillation (9.51 cpd) corresponding to this mode is only seen in about half the spectra in Figs. 2 and 3. When it is seen, most strongly at CC, it appears to be a component in a broad and probably multiple peak. Although the calculated and observed distributions agree fairly well, we made no entry in Table 3 because no clear phase progression could be discerned in the 1962–63 interstation comparisons.

f. Mode 10.55 cpd (first transverse mode, f in Fig. 3)

The large, apparently single peaks at 10.94 cpd at MI, WA, CW, HO and LU (Figs. 2 and 3) are clearly identified with this mode, which displays (Fig. 6b) an extensive negative amphidrome in the southern one-third of the basin and eight positive amphidromes (four of which are in Green Bay) with generally negligible elevation range elsewhere. The comparison in Table 3 is interesting. Because of the strong excitation of this mode—it was interpreted as a transverse standing oscillation by Comstock (1872a, b) in advance

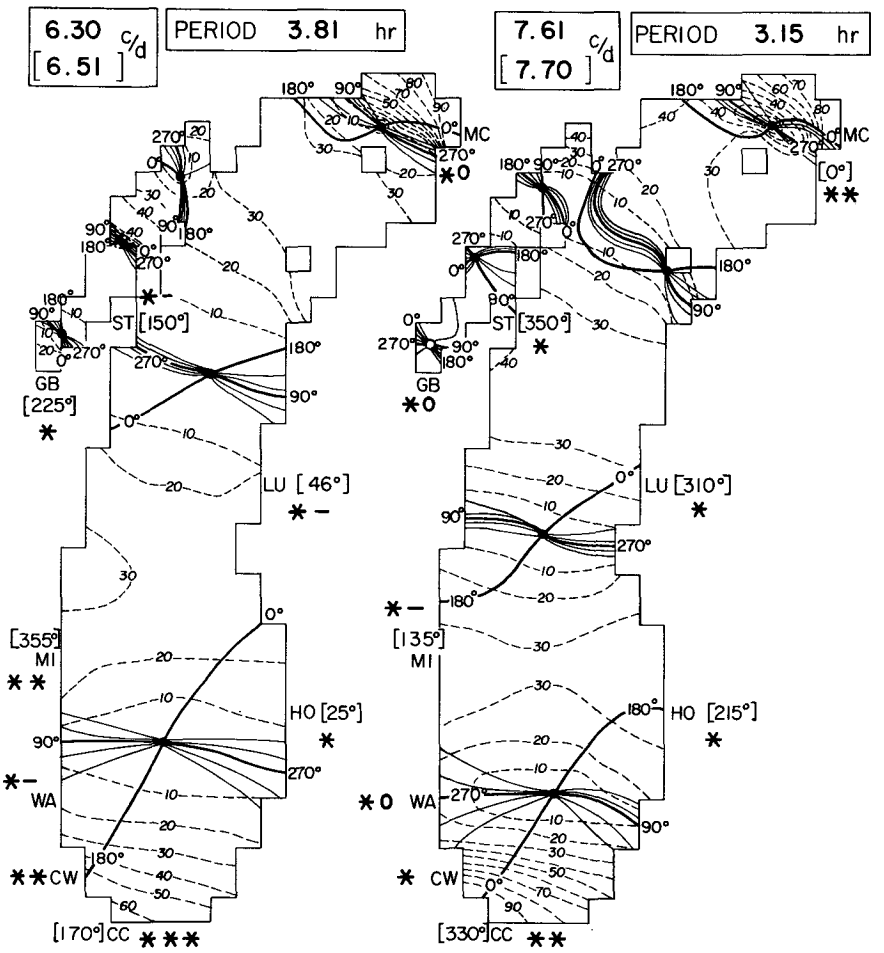

FIG. 5. As in Fig. 4 except for the third and fourth longitudinal modes.

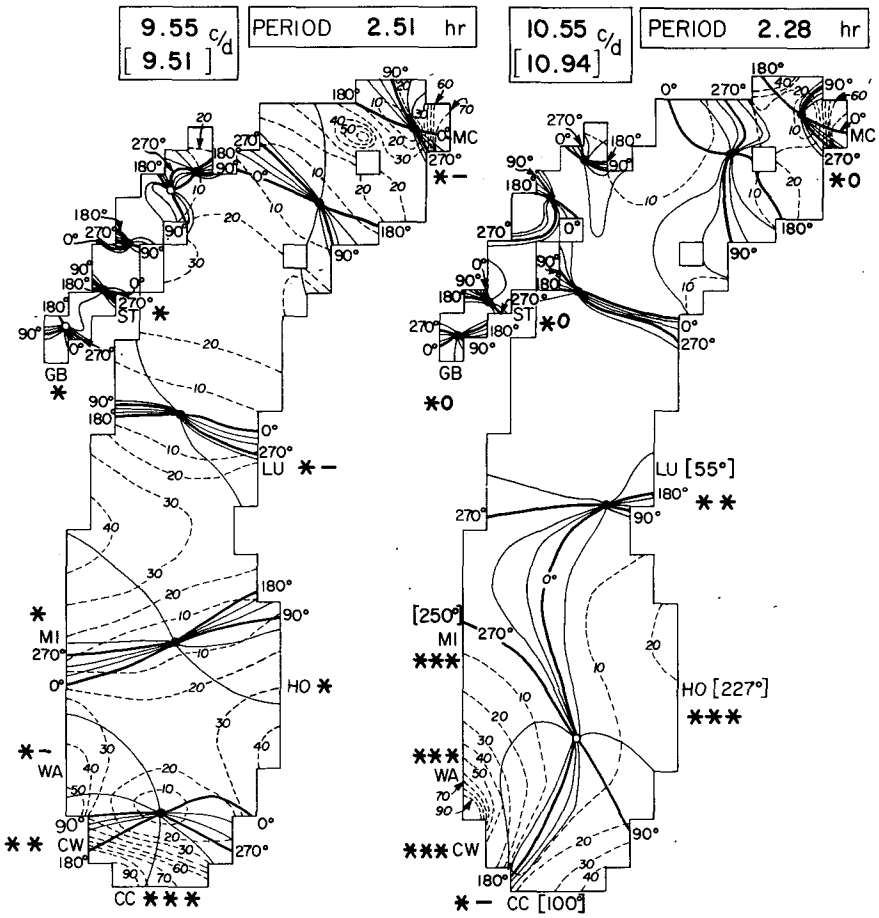

FIG. 6. As in Fig. 4 except for the fifth longitudinal mode (9.55 cpd) of the main Lake Michigan basin and the mode (10.55 cpd) identified as the first transverse oscillation of the southern part of the basin.

of Forel's better-known seiche interpretations for Lac Leman—the oscillation is conspicuous at several stations, including MI and LU, for which the *relative* calculated amplitudes are low. Agreement in phase progression is good for some stations but not (as often appears to be the case) at GB and, more significantly, not at HO and LU. A clear explanation of this discrepancy is now lacking, but it may be linked with the fact that HO and LU are the only two recorders placed in small lakes connected to the main basin through long, narrow shipping channels. The recorded levels may therefore not be in phase with lake levels at this and higher frequencies.

g. The remaining modes

A complete listing of the first 13 normal mode frequencies, calculated with rotation, is given for the main basin in Table 1. Four of the remaining modes (8.86, 11.96, 12.61 and 13.61 cpd) can be unambiguously identified with spectral peaks in Figs. 2 and 3, as indicated in Table 1, using the elevation comparison procedure of Table 3. (We intend to describe the structures of these modes in a Special Report of the Center for Great Lakes Studies, University of Wisconsin-Milwaukee.) Since the spectral expansions in Eq. (5) are limited to 50 terms, truncation errors in the higher rotating modes become increasingly serious. Therefore, our comparisons for main basin modes do not go beyond 14 cpd.

5. The Green Bay normal modes

a. Frequency calculations using coarse and fine grids

It is of particular interest to examine the modes of Green Bay. In studies of bay (and gulf) oscillations, the precise location of the mouth, connecting the bay to an open water body, is in general not obvious *a priori*. In our calculations, the numerical grid covers the Lake Michigan and Green Bay combined system, even though the Bay is resolved in a crude manner. As a consequence, the calculations yield information about the approximate location of the mouth since the Green Bay modes form a subset of the total modes obtained. These calculations also show, not surprisingly, that the

shape of the line defining the mouth is a curved line, lying outside the topographic entrance and changing position with different modes.

Among the various modes of oscillation of a bay, the lowest has only one nodal line at the mouth and none in the interior of the bay. The frequency of this mode tends to zero as the mouth is closed, and it has no counterpart in any of the modes of a closed basin in contrast to the higher modes of a bay, all of which can be made to correspond to modes of a closed basin. In tidal terminology this lowest mode is the co-oscillating mode and in acoustic terminology the Helmholtz mode.

As noted earlier, the lowest normal mode of the Lake Michigan-Green Bay system is the co-oscillating Green Bay mode, with elevation range confined almost entirely within the Bay and with less than 10% of relative elevation range elsewhere. The structures computed without and with rotation, show an arc-shaped nodal line and an arc-shaped amphidromic region, respectively (Fig. 7a), lying well outside the mouth of the Bay. The periods (>15 h) initially determined by these calculations are in conflict with spectral evidence (Mortimer, 1965; Mortimer and Fee, 1976) that the observed period of the lowest Bay mode lies between 10 and 11 h.

The numerical grid covering the Lake Michigan-Green Bay system was chosen, as shown in Fig. 1, to yield a satisfactory representation for the main basin of Lake Michigan. Obviously, the resolution of the Green Bay characteristics by this grid turned out to be rather poor. To test whether this discrepancy arises because the grid is too coarse or because it is poorly aligned to the Bay shoreline, we carried out two sets of normal mode calculations for the bay alone, without rotation and with a nodal line imposed outside the mouth in the position determined by the nonrotating calculation for the first mode. In one set [(b) in Table 4], the same grid spacing (14.4 km) was used, but the grid was aligned 32° east of north, parallel to the main axis of the Bay. In the other set of calculations [(c) in Table 4] a finer grid spacing (7.2 km 41° east of north; see Fig. 8) was adopted. The results are presented in Table 4 because of their methodological interest. Column 1 lists the frequencies of the Green Bay modes

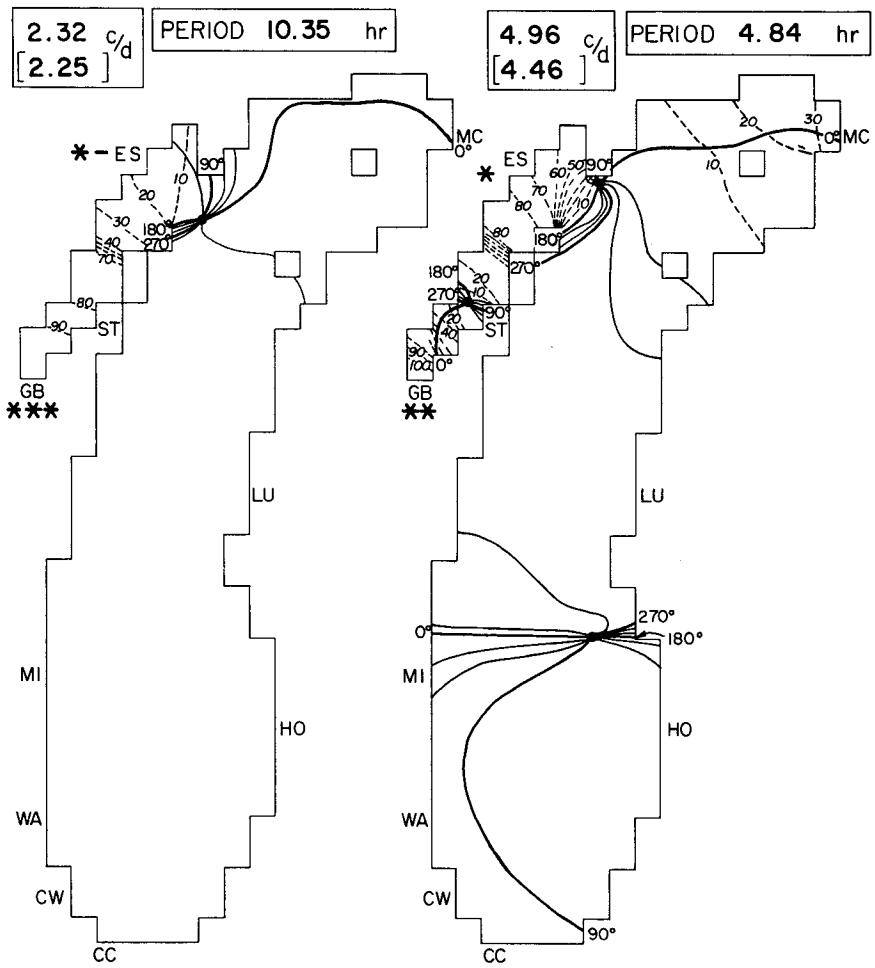

FIG. 7. As in Fig. 4 except for the first and second Green Bay modes.

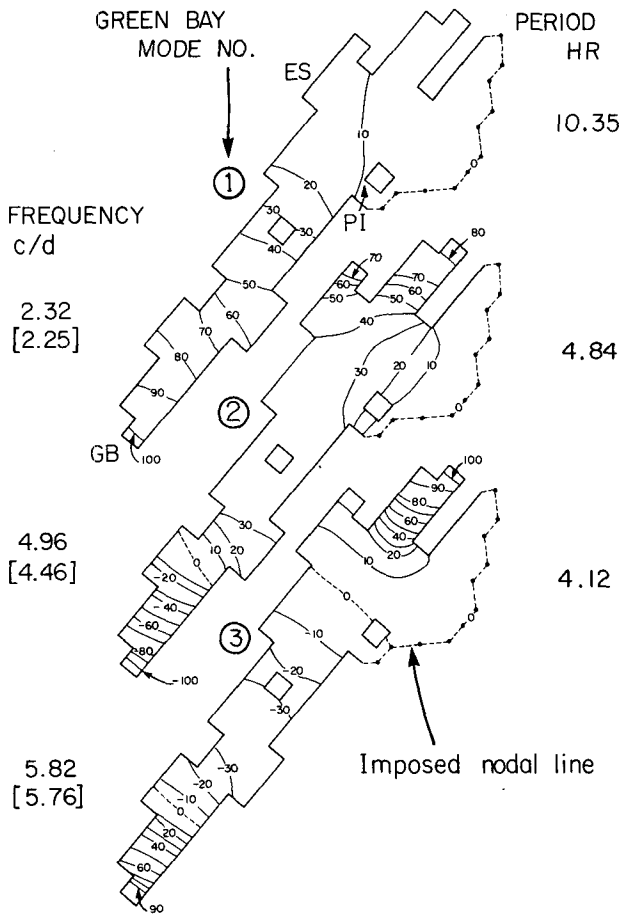

FIG. 8. Frequency, period and distribution of elevation range calculated from velocity potential (without rotation) for the first three modes of Green Bay, using a "fine" grid of 7.2 km spacing aligned 41° east of north, and with a nodal line imposed outside the Bay mouth. The arc-shaped nodal line is that derived for the first Bay mode, calculated using the "coarse" (Fig. 1) grid without rotation. The bracketed "observed" frequencies are those of Table 4, identified with the calculated modes. The elevation ranges are relative to +100 at that grid point which exhibits the highest elevation range for the mode in question.

initially obtained using the coarse grid applied to the whole basin, without rotation and with no nodal line imposed at the mouth. For comparison with the calculated frequencies listed in column 3, spectra of Green Bay water level fluctuations at three stations are assembled in Fig. 9. The two lower spectra GB (1961) and GB (1963 under ice cover) are equivalent to those in Figs. 2 and 3, being based on about 60 days of 15 min averages.

When compared with the frequencies of observed oscillations listed in column 4 in Table 4, column 1 shows a poor fit, while column 3 generally shows the best fit. These results may be attributed not only to the coarseness of the grid but also to the unnatural boundary condition for the transport on a misaligned, zig-zag boundary. However, the imposed nodal line (Fig. 8) may be unrealistic for the higher modes.

b. The first Bay mode

All the available spectra show most of the power concentrated in a large broad peak with two or sometimes three distinct summits, the highest at the semidiurnal tidal frequency, 1.95 cpd. There is a second summit near 2.7 cpd, the first main basin mode, and usually a third summit near 2.2 cpd representing the lowest Bay mode. Because of the closeness of their frequencies to the Bay mode, the semidiurnal tide and the first main basin mode force the Bay into strong resonance. Proof that the frequency of the Bay mode must lie between 1.95 and 2.7 cpd is afforded by the phase relationships. Mortimer and Fee (1976) observed that "MC leads GB by 35° and 175° at 1.95 and 2.7 cpd, respectively." The small but distinct summits at 2.2 cpd in two spectra in Fig. 9 are therefore taken to represent the first Bay mode. As Fig. 7a shows, the relative elevation range of that mode is low (<10%) in the main basin, but there is evidence of this oscillation as a small but persistent sub-peak or "shoulder" on the high-frequency side of the tidal peak in spectra of several main basin stations.

c. The second Bay mode

There is also a large second mode peak in all spectra in Fig. 9. Johnson (1963) also found 5 h oscillations to be common at ES. This peak is broad and probably double, one component (the right-hand summit) coinciding with the main basin second mode. This leaves the other summit near 4.5 cpd as candidate for the second Bay mode, but at a lower frequency than shown in Table 4, column 3. A possible reason for this dis-

TABLE 4. Computed and observed frequencies (cpd) of the first four Green Bay normal modes. Computations were made *without* rotation and were based on the following grids:

(a) The original grid (Fig. 1) with 14.4 km spacing, applied to the whole basin.
(b) A grid with 14.4 km spacing aligned 32° east of north.*
(c) A grid with 7.2 km spacing aligned 41° east of north* (the equivalent period is in parentheses).

Frequencies of the observed Green Bay oscillations (see text and Fig. 9) are listed in column 4. Structures of modes 1 and 2, with rotation, are shown in Fig. 7.

	Computed frequencies				
Green Bay mode number	(1) Original coarse grid (cpd)	(2) Aligned coarse grid (cpd)	(3) Fine grid (cpd)	Period corresponding to col. 3 (h)	(4) Observed oscillation frequency (cpd)
1	1.56	2.01	2.32	(10.35)	2.25
2	4.00	4.05	4.96	(4.84)	4.46
3	5.27	4.88	5.82	(4.12)	5.76
3	7.30	7.27	6.91	(3.47)	7.01

* Grids (b) and (c) were applied to the Bay only, with a fixed modal line outside the mouth (see Fig. 8). The number of ϕ points was 25 for (a) and (b) and 108 for (c).

crepancy is seen in Fig. 7b. The nodal "line" (the 90°–270° phase line) of the second mode extends further into the main basin than does the 90°–270° line of the first mode. Imposition of the first-mode nodal line in the second mode calculation may therefore have given a frequency result which was too high. On the evidence of the spectra, the second mode frequency is taken to be near 4.5 cpd.

d. The third and fourth Bay modes

The third Bay mode is represented by a small peak near 5.8 cpd in the 1961 GB spectrum (Fig. 9). It may also account for the "shoulder" on the second mode peak in the 1963 spectrum, but it is absent at ES. Fig. 8 shows only 20% elevation range at that station, in contrast to the fourth mode (not illustrated) which shows a relatively large amplitude in Little Bay du Noc, in which ES is situated. A distinct peak at this frequency is in fact seen at ES near 6.9 cpd, alongside another distinct peak at the frequency of the third main basin mode at 6.5 cpd. The fourth Bay mode is also represented by a subsidiary peak in the 1963 GB spectrum, but is not distinct in the 1961 spectrum.

6. Summary

Theoretical calculations made to determine the periods and structures of the two-dimensional normal modes of Lake Michigan indicate that the spectrum of normal modes contains some that are dominant in the main basin of Lake Michigan and some that are dominant in Green Bay. Our numerical grid gave rather poor resolution for the Green Bay modes. Hence, using the information (from this "crude" grid model) about the location of the mouth for the co-oscillating Green Bay mode, additional calculations were made for Green Bay alone using the same grid interval as before but with the major axis aligned along the length of the bay and a finer grid of half the previous size. Both these procedures yield a marked improvement in results.

Focusing attention on the gravitational modes, detailed comparisons were made of the periods and structures obtained from theory and observations. The observed characteristics were displayed in spectra of water level fluctuations at several stations around the Lake Michigan basin. The spectra indicate a high degree of complexity in the free surface responses. However, it was possible to identify several of the lowest modes of the Lake and to obtain satisfactory verification of the theoretical results. Verification of the higher modes becomes progressively more difficult because their structures increase in complexity and the resolution of the observational network (11 shore-based stations, Fig. 1) is limited.

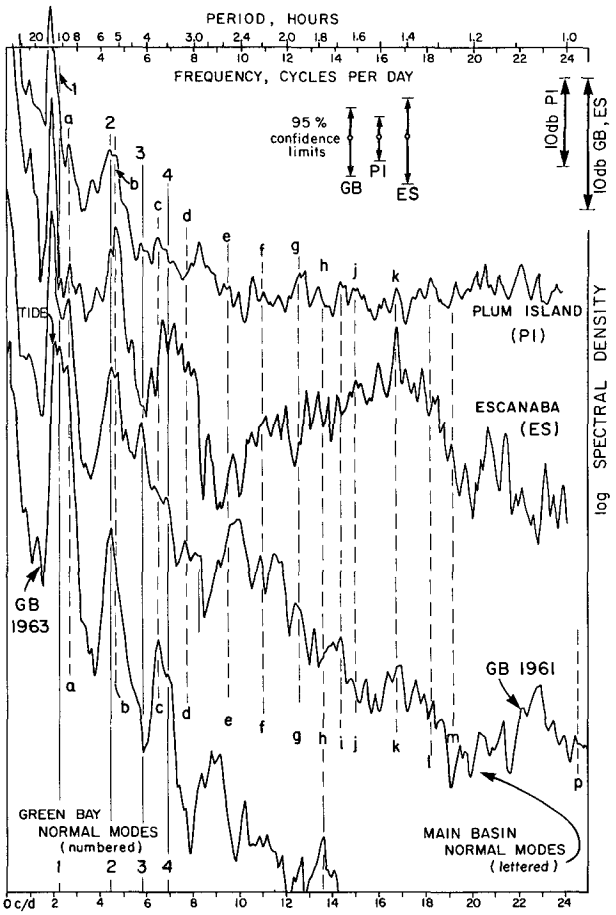

FIG. 9. Spectra of water level fluctuations based on two months of 15 min average levels at GB, Green Bay City (July–August, 1961; January–February, 1963, under ice); 44 days of 30 min average levels at ES, Escanaba (August–October, 1953); and three months of 30 min average levels at PI, Plum Island (August–November, 1969). Numbered, unbroken vertical lines are placed at the frequencies identified as those of "observed" oscillations corresponding to the Green Bay modes, defined in the text. Lettered, broken vertical lines are those identified with Lake Michigan main basin modes, transferred from Figs. 2 and 3.

Acknowledgments. Verification of our normal mode calculations would not have been possible without the water level records generously provided by the U. S. Lake Survey (then U. S. Army Corps of Engineers, F. Wayne Townsend, Chief, Hydrology Branch); the Illinois Division of Waterways (records for stations CW and WA); and the late R. L. Johnson (Michigan Department of Health, records from Escanaba). Our thanks are also due to C. Hutchings and to E. J. Fee for computing the spectra. The work was performed while Mortimer and Schwab were supported by the Center for Great Lakes Studies, University of Wisconsin-Milwaukee; and we are indebted to R. J. Ristic for painstaking preparation of the figures, and to D. F. Mraz for records from Plum Island.

REFERENCES

Comstock, D. B., 1872a: Irregular oscillations in surface of Lake Michigan at Milwaukee. *Ann. Rep. Survey Northern and Northwestern Lakes*, Appendix B, 14–15, *in* Report Sec. of War to 3rd Session 42nd Congress, Vol. 2., Washington, D. C. [U. S. Govt. Printing Office].

——, 1872b: Tides at Milwaukee, Wisconsin. *Ann. Rep. Survey Northern and Northwestern Lakes*, Appendix A, 9–14, *in* Report Sec. of War to 3rd Session 42nd Congress, Vol. 2., Washington, D. C. [U. S. Govt. Printing Office].

Defant, A., 1961: *Physical Oceanography*, Vol. 1. Pergamon Press, 729 pp.

Johnson, R. L., 1963: Tides and seiches in Green Bay. *Proc. 6th Conf. Great Lakes Research*, Publ. 10, Great Lakes Res. Div., University of Michigan, 51–58.

Mortimer, C. H., 1965: Spectra of long surface waves and tides in Lake Michigan and at Green Bay, Wisconsin. *Proc. 8th Conf. Great Lakes Research*, Publ. 13, Great Lakes Res. Div., University of Michigan, 304–325.

——, and E. J. Fee, 1976: Free surface oscillations and tides of Lakes Michigan and Superior. *Phil. Trans. Roy. Soc. London*, **A281**, 1–61.

Platzman, G. W., 1972: Two-dimensional free oscillations in natural basins. *J. Phys. Oceanogr.*, **2**, 117–138.

——, 1975: Normal modes of Atlantic and Indian Oceans. *J. Phys. Oceanogr.*, **5**, 201–221.

Proudman, J., 1916: On the dynamical equations of the tides. *Proc. London Math. Soc.*, 2nd Ser., **18**, 1–68.

Rao, D. B., 1966: Free gravitational oscillations in roating rectangular basins. *J. Fluid Mech.*, **24**, 523–555.

——, and D. J. Schwab, 1976: Two-dimensional normal modes in arbitrary enclosed basins on a rotating Earth: Application to Lakes Ontario and Superior. *Phil. Trans. Roy. Soc. London*, **A281**, 63–96.